Wear and corrosion of silicon nitride rolling tools in copper rolling

I. Khader[*] [a,b], A. Hashibon[a], J.-M. Albina[a], A. Kailer[a]

[a]*Fraunhofer Institute for Mechanics of Materials IWM, Freiburg, Germany.*

[b]*Karlsruhe Institute of Technology, IZBS – Institute for Reliability of Components and Systems, Karlsruhe, Germany*

Date Line

Abstract

For hot rolling applications it is essential to have materials with excellent high-temperature properties. Silicon nitride combines the properties optimum relevant to such high demanding applications, including thermal shock resistance, low density, high elastic modulus and low coefficient of friction. However, its chemical stability and corrosion resistance when brought into contact with copper at high temperatures and pressures is still a topic of research. In this study the corrosion and wear behavior of silicon nitride applied in rolling copper wires is investigated. For this purpose laboratory-scale wire rolling experiments were carried out and a series of atomistic simulations based on density functional theory DFT calculations were performed. The goal here is to identify the factors leading to the corrosion of silicon nitride in copper wire rolling, and to show how silicon nitride rolls differ from conventional steel rolls in terms of adhesion with copper. The experimental and numerical results were then compared with failed silicon nitride specimens tested in an industrial wire-rolling mill. The experimental results showed no signs of corrosive pitting or fracture on the rolls, however, indicated remarkable tribochemical wear especially in the presence of a lubricant. The numerical computations showed that the affinity of silicon nitride to copper is low in comparison to the affinity of ferrous-based tools to copper. The DFT calculations also explained one of the major wear-assisting mechanisms in this process. Finally, the failure of the industrial ceramic rolls was clarified by relying on FIB-SEM and EDX analyses.

Keywords: Silicon nitride, copper, corrosion, wire rolling, DFT, adhesion.

1. Introduction

In the field of copper wire rolling, steel-based tools are commonly used to roll the wires. High wear, chemical corrosion and oxidation at elevated temperatures and excessive adhesion to metals are widely

[*] Corresponding author. Tel.: +49 761 5142429; fax: +49 761 5142403.
E-mail address: iyas.khader@iwm.fraunhofer.de (Iyas Khader)

encountered in steel-based materials. The complication of debris formation resulting, eventually, in wear particles penetrating the workpiece surface, remains an unresolved issue. Adhesive wear significantly reduces the lifetime of the work-rolls and moreover, affects the quality of the workpiece by compromising surface tolerances and introducing wear particles in the work zone. Brittle oxide layer formation on the roll surface and the subsequent detachment of particles has been reported to result in similar undesirable consequences. During manufacturing, copper wires are quite often drawn into very fine cross sections (ca. 25 μm). The presence of debris in the wires, from preceding rolling steps, can easily cause rupture at such small cross sections. Engineering ceramics, such as silicon nitride, have already shown wide success when applied in several metal forming applications. Several recent studies have established that silicon nitride wire rolling tools were applied with increased lifetimes in comparison to conventional rolls, especially in finishing blocks of industrial rolling mills **[1-3]**.

The application of wear resistant and chemically stable materials at high temperatures, such as silicon nitride, might offer an attainable remedy. However, the research work treating the application of silicon nitride tools in rolling copper is fragmentary. Likewise, the available literature on experiments treating the interaction between copper and silicon nitride has so far presented contradicting results.

The behavior of silicon nitride in contact with different metals is diverse. Focusing on copper, previous studies have shown that copper alloys, such as bronze, when brought into sliding contact with silicon nitride, even at low speeds and low temperatures, produce tribofilms and traces of very fine debris on the surface of the ceramic **[4]**. This has been attributed to chemical interaction with the surface of silicon nitride. These chemical interactions may also be intensified by high contact temperatures. Other studies argued that silicon nitride shows grain boundary phase damage when brought in contact with copper. Nonetheless, studies examining rolling pure copper with silicon nitride work rolls are scarce.

A non-wetting behavior between molten copper and hot-pressed silicon nitride (HPSN) was independently observed by Klein et al. **[5]** and Sangiorgi et al. **[6]**. In a later study, Sangiorgi et al. **[7]** suggested a chemical reaction between copper and silicon nitride that might lead to corrosion induced surface damage; such corrosion was documented in several samples and it took the form of surface pitting. This phenomenon was explained by chemical attack on the secondary phase and the decomposition of the grain boundary phase of silicon nitride. It was proposed that the corrosion is dependent on the type and amount of the secondary phase and the chemical composition of silicon nitride (i.e., sintering additives).

Research findings on applying Si_3N_4-based tools in direct contact with pure copper and copper alloys are very limited. An exception to this is the study presented by Wötting et al. **[8]**. The authors presented cases, in which silicon nitride rolls were applied in caliber rolling of copper wires at elevated temperatures. It was reported that the friction at the tool/workpiece interface as well as the high temperatures associated with the process can augment the tribomechanical and tribochemical effects; thus in turn accelerate the initiation of damage. The argument of a chemical reaction taking place between copper and silicon nitride and leading to the formation of copper silicides (e.g., Cu_3Si and Cu_4Si) was also proposed **[9]**.

One of the key issues in wire rolling is the quality of the metal surface produced, which in turn, is strongly affected by the interaction and nature of adhesion between the wire metal and the roll material. This is particularly important since the metal flows into the roll gap at high temperatures in a solid state, and hence its reactivity with the die material is expected to be high. This may also easily lead to undesirable results upon cooling, such as strong sticking, and elevated surface roughness.

Atomistic simulation techniques have proved to be a useful tool for investigating the degradation mechanisms in crystalline materials. These methods (e.g., molecular dynamics or first-principles methods) play a significant and complementary role to experiments by providing valuable information on the detailed atomic and electronic structure at the interface. To date, the available experimental models for predicting the adhesion affinity are limited to liquid-metal/oxide interfaces, e.g., through sessile drop experiments **[10]**. Unfortunately, very little is known about interfaces involving non-oxide ceramics, which are commonly used as tribological coatings **[11]**.

At the interface between a metal and a ceramic, complex bonding is formed, which requires an atomistic modeling approach capable of accurately describing the ionic or metallic interactions in each of the phases separately, in addition to the mixtures of covalent, metallic and ionic bonding in the interface region. A first-principles treatment based on the density functional theory (DFT) **[12,13]** would therefore be most appropriate for examining the nature of local bonding and adhesion. Indeed this approach has proved to be useful for studying adhesion between metal films and ceramic substrates in numerous systems **[14-17]**, for recent reviews cf. **[18,19]**.

In the present study, laboratory-scale wire rolling experiments supported by a series of atomistic density functional theory (DFT) calculations are carried out to investigate the suitability of silicon nitride rolls in rolling high purity copper wires, and an explanations on the damage patterns observed during the testing of the rolls is proposed.

The paper is divided into three parts: In the first part (section 2), the experimental setup and procedures are described. The second part treats the theoretical DFT calculation method and system modeling techniques adopted throughout this study. The results of both experimental and numerical analyses are presented in section 4. Part three (section 5) presents a case study from the industry. Thereafter, a discussion relating the experimental and theoretical findings is presented in section 6. Finally, section 7 concludes this paper with a summary.

2. Experimental procedure and setting

2.1. Ceramic work-rolls and wire material

The ceramic rolls were prepared from a commercial silicon nitride powder (Si_3N_4, CeramTec AG, Germany). The powder conditioning and production of green bodies by cold isostatic pressing (CIP) was carried out at the Institute for Ceramics in Mechanical Engineering (IKM), Karlsruhe Institute of Technology (KIT). Subsequent sintering was carried out by CeramTec AG, Germany. This grade of silicon nitride (labeled SL 200 BG) contains approximately 3 wt.% Al_2O_3 and 3 wt.% Y_2O_3 as sintering additives. The microstructure consists mostly of β-grains of average diameter ca. 1.5 µm and average aspect ratio of 3 to 5 **[20].** The structure contains ca. 12 vol.%

intergranular glassy phase. More details concerning the sintering process are given in **[21]**. The machining of the rolls was carried out by BeaTec GmbH, Germany. The rolls (outer diameter: 55 mm) were ground to an average roughness of $R_a < 0.5$ µm. Two oval rolling calibers (grooves) were machined on the surface of the rolls (width=3.52 mm, depth=0.51 mm), then polished down to an average roughness of $R_a < 0.4$ µm. It is worth mentioning that the specimens were surface-ground and polished circumferentially. The dimensions of the ceramic rolls are given in **Figure 1**.

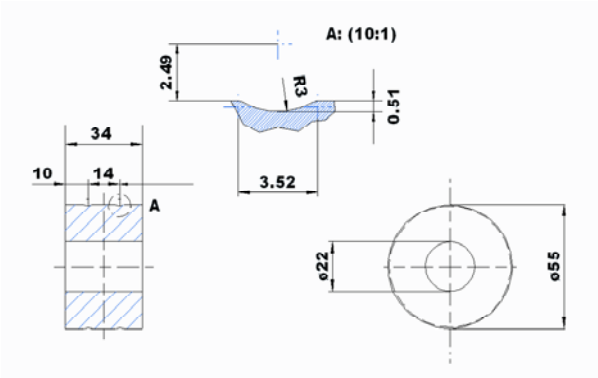

Figure 1. Dimensions of the silicon nitride rolls (units: mm)

Oxygen-free (< 5 ppm) copper wire (Cu-OF1, Nexans Deutschland Industries, Germany) was used for the hot rolling experiments. The amount of additional elements beside Cu in the wire material is given in **Table 1**.

Table 1. Typical additional elements (Cu excluded) in ppm found in Cu-OF1 as provided by the supplier

Ag	As	Bi	Fe	Pb	S	Sb	Se	Te
8.0	1.0	0.4	1.0	1.0	4.0	1.0	0.5	1.0

A mineral-oil-based (UNOPOL G 600, Bechem, Germany) cooling lubricant (concentration 5% in 95% water) was used in the lubricated experiments. This lubricant is commercially available and used in copper wire drawing.

2.2. Wire rolling test rig

A wire rolling test rig was constructed at the Fraunhofer Institute for Mechanics of Materials IWM to carry out hot rolling experiments using ceramic rolls. A schematic drawing of the test rig is shown in **Figure 2**.

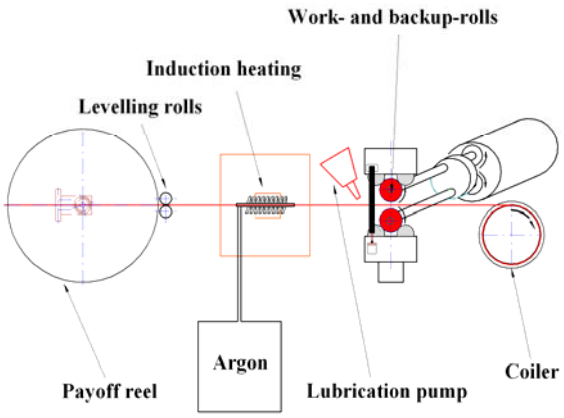

Figure 2. Roll test rig for hot wire rolling using silicon nitride rolls. The rolls are installed in a cluster mill configuration

As illustrated in **Figure 2**, the wire uncoils from a payoff reel (uncoiler), which also controls the back tension using a braking system. After passing through a set of levelling rolls, the wires pass through a ceramic pipe and into an induction heating unit, which heats the wires under a stream of inert gas (argon). Using an inert gas reduces metal oxidation at high temperatures and consequently, ensures better metal/ceramic contact. Shortly before reaching the roll gap, the temperature of the wire slightly cools down reaching the desired rolling temperature (T_i). The wire is pulled into the roll gap, at a predefined feed rate, by traction forces arising from friction with the surfaces of the rolls. The profile of the roll gap generated by both calibers, on the set of work-rolls, gives the wire its final oval cross section. The applied compressive load, which maintains a preset reduction ratio, is constantly monitored and adjusted by means of fixed-displacement-variable-load controls of the servo-hydraulic universal test frame. After exiting the roll gap, the wire wounds around a delivery reel (coiler), which additionally controls the front tension by adjusting the torque. The cross-sectional reduction and the applied load are electronically controlled and monitored in the testing machine. The temperature is monitored by means of pyrometers which were calibrated by comparing their readings with outputs from thermocouples. Finally, the wire velocity and feed rate are controlled via rotational sensors located at the leveling rolls and the work-rolls.

3. Computational first-principles method and atomistic structure models

The DFT calculations were performed to estimate the adhesion between Cu and the roll through the computation of the ideal work of separation, W_{sep} for simple model systems. The ideal work of separation W_{sep}, is defined as the energy difference per unit area between an interface system and one where the two surfaces are completely separated. W_{sep} does not include irreversible effects such as plastic deformation and interaction with the environment. It specifies the amount of energy expenditure needed in a system to cause a separation of the interface (mechanical failure) **[15]**. The work of separation calculated in this manner gives direct information on the adhesion and chemical bonding at the interface **[22]**.

3.1. The first-principles DFT calculations method

The computational first-principles method is based on the density functional theory (DFT) **[13]** and the local-density approximation for exchange and correlation (LDA) **[23,24]** employing norm-conserving pseudopotentials **[25]** and a mixed basis of localized orbitals and plane waves **[26-29].** The pseudopotentials were constructed from all-electron valence states for free atoms according to Vanderbilt **[30]**. Plane waves up to the cutoff energy E_{pw}=16 Rydberg were used (1 Rydberg=13.606 eV). A 2×2×1 Monkhorst-Pack k-point mesh **[31]** and a Gaussian broadening of 0.2 eV were used for the metal/ceramic interfaces. The k-point mesh was increased to 4×4×2 for the metal/metal interfaces. This setup was found to be sufficient for well converged results.

3.2. Atomistic interface models

The work of separation is calculated for three cases, namely Cu on Si_3N_4, Cu on SiO_2, and Cu on γ-Fe. Silica is found in the secondary phase of the silicon nitride material system. It also forms on the surface of the rolls at high temperatures due to the oxidation of Si_3N_4 and/or the sintering additives (e.g., Al_2O_3, Y_2O_3) [**32**]. In addition to the calculation of W_{sep} between Cu and Si_3N_4 and between Cu and SiO_2 as composites of the ceramic tool, the adhesion between Cu and austenite γ-Fe was investigated as a model case of steel rolls. This simultaneous approach enables drawing conclusions on the suitability of conventional ferrous-based (i.e., steel-based) tools in comparison to ceramic-based (i.e., silicon nitride) tools.

There are two well known polymorphs of silicon nitride cf. e.g., **[33],** namely the α-Si_3N4 and β-Si_3N_4 phases. The α-phase is synthesized at low temperatures, while the more stable β-phase is obtained by a transformation of the α-phase into β-phase at elevated temperatures during sintering. Both of the polymorphs have the same underlying hexagonal structure, and only differ by the stacking sequence along the z-axis. The α-phase has a space group $P3_{1c}$ with 28 atoms in the unit cell, while the β-phase has the space group $P6_3/m^3$ with 14 atoms in the primitive unit cell. Only the stable β-phase, which has half the number of particles in the unit cell (refer to section 2.1 for experimental material), was considered here. In particular, since the basal (0001) surface of both systems is similar, it is expected that the results for the adhesion on the surface of both polymorphs are also very similar.

For the case of the interfaces between Cu and SiO_2, the most stable polymorph, namely α-quartz was used. Even though during rolling at high temperatures and pressures, other crystalline or amorphous polymorphs of silica may form. This is justified since our main focus is to investigate the effect of local bonding on the adhesion, which should not drastically vary with the structure. Even for the case of amorphous silica, which has no long range order, on length scales comparable to a Si-O bond, it is nearly perfectly ordered, i.e., the bond length does not vary appreciably from the crystalline phase **[34]**.

The DFT calculations, although accurate, are computationally intensive and therefore, limited to small systems. Hence, in this study the focus was on simple coherent systems, and atomically sharp interfaces. Since the orientation relationship between Cu and α-Si_3N_4 is unknown, the interfaces formed between Cu (111) and the (0001) basal plane of crystalline β-Si_3N_4 and α-SiO_2 were considered in this work. For the calculations, the experimental lattice parameters for β-Si_3N_4, a_0=7.607 Å **[35]** and a_0=4.916 Å **[36]** for α-SiO_2 were adopted. For γ-Fe, a_0=3.409 Å **[37]** was used.

The interface systems are modeled by slab supercells, consisting of 4 or 3 (111) planes of Cu on the (0001) surface of Si_3N_4 and SiO_2, respectively. In the Cu/Fe interface model, the supercell contained 5 (111) planes of Cu on 4 (111) planes of face-centered cubic (fcc) γ-Fe. Periodic boundary conditions parallel to the surface and normal to the interface are applied. In the case of Si_3N_4, and SiO_2, a vacuum region was inserted on one side of the substrate, to obtain one interface. In the case of the Cu/γ-Fe system, no such vacuum region was inserted; hence, two interfaces were modeled in the system. In all cases, the in-plane lattice constant of Cu was fixed to the lattice constant of the substrate (coherent interfaces), while the out-of-plane lattice parameter is free to adjust to the value that minimizes the free energy of the system. The supercell used for the Cu/Si_3N_4 is shown in **section 4.2**.

4. Results

4.1. Experimental results

Immediately after running the hot rolling experiments, obvious coloration was observed on the surfaces of the calibers (rolling grooves). Under unlubricated conditions, stereo microscope examinations (**Figure 3**) of the rolls indicated metallic transfer layers on the surfaces of the calibers. The material transfer initially generated metallic layers on the silicon nitride surface. After reaching a steady state (rolling approximately 2000 m, alternatively 11.5×10^3 contact cycles), the buildup took the form of small sparse adherent particles on the surface of the rolling calibers as shown in **Figure 3b**. The lubricated experiments resulted only in coloration of the calibers without observing buildup layers on the ceramic surface.

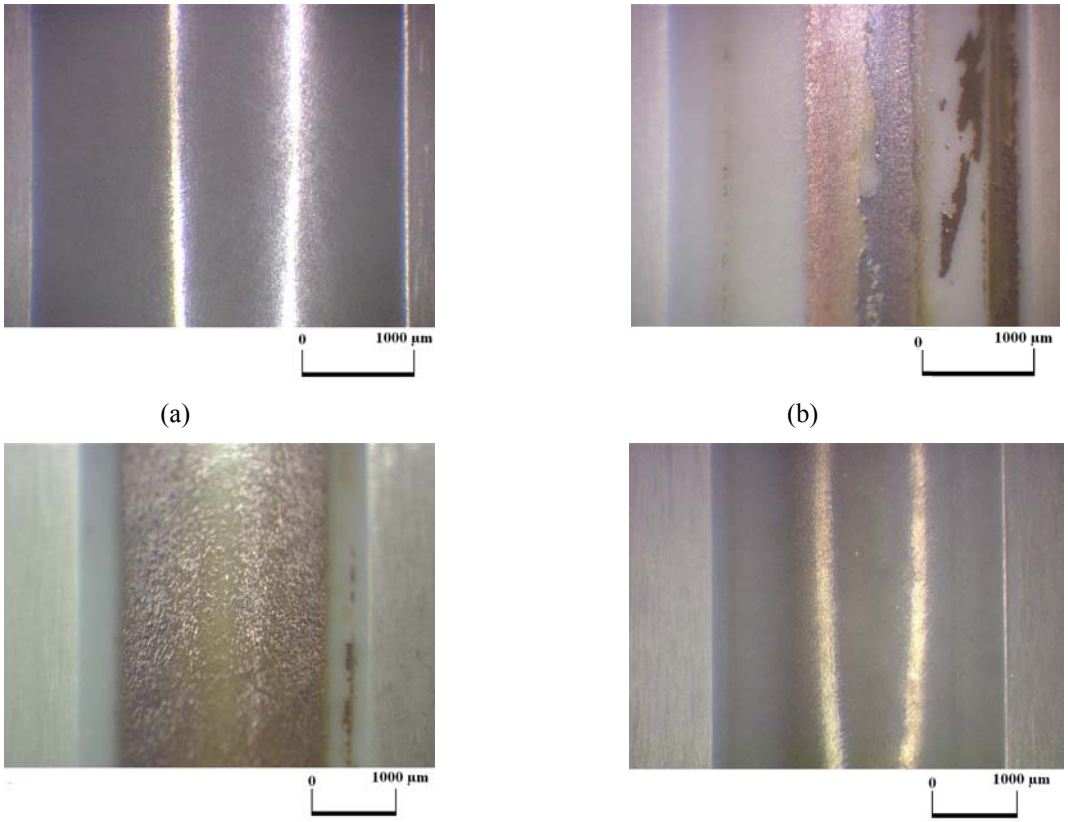

Figure 3. Optical micrographs showing the caliber surface in: (a) a virgin-state specimen; (b) after the first few cycles without lubrication; (c) after rolling 2000 m without lubrication; (d) after rolling 2000 m with lubrication

A contour measurement, shown in **Figure 4**, illustrates the profile variation of the caliber due to the metallic transfer layers. The contour measurement shown in **Figure 4**, illustrates that the transfer layer superposes on the surface of the ceramic.

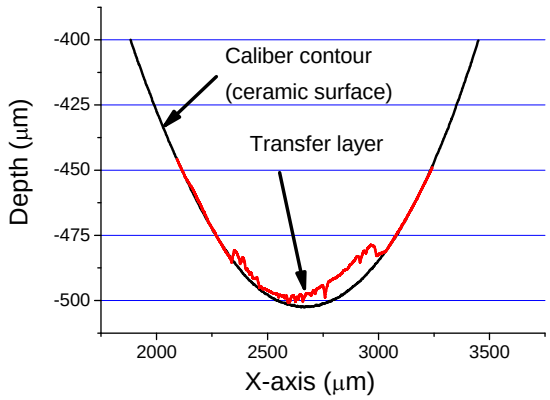

Figure 4. Caliber contour measurement showing the effect of transfer layers on the roll surface

An energy-dispersive X-ray spectroscopy (EDX) quantitative analysis was carried out in order to analyze the composition of the transfer layers. **Figure 5** shows an SEM image of the caliber surface and the metallic agglomerates on the surface, whereas a summary of the EDX analysis is shown in **Table 2**.

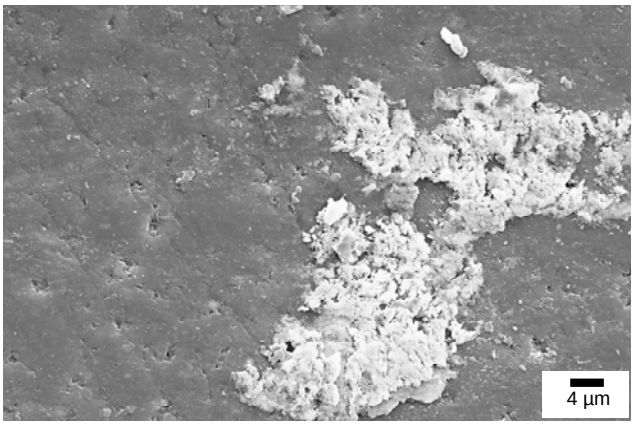

Figure 5. SEM micrograph showing the surface of the caliber after hot-rolling 2000 m of copper wire without lubrication and the corresponding EDX quantitative analysis

Table 2. Summary of an EDX quantitative analysis after rolling 2000 m of copper wire without lubrication

Element	**Source**	**Mass %**	**Atom %**
O	Oxides and sintering additives	13	32
Al	Sintering additives	2	2
Si	Si_3N_4/SiO_2	18	25
Cu	Cu-wire	62	38
Y	Sintering additives	1	1
Au	Sputtering	15	2

The EDX analysis revealed copper content with the highest mass percent. It also confirmed the presence of silicon, yttrium and aluminum, which originate from the silicon nitride material composition. Additionally, oxygen was detected, which partially stems from sintering additives and also suggests the formation of copper oxides and/or silicon oxide on the surface of the caliber.

To study the surface of the silicon nitride specimens below the transfer layers, SEM surface examinations and roughness stylus profilometry were carried out after chemically etching the metallic transfer layers using a

solution of 53% HNO_3. This acidic solution does not chemically attack the ceramic surface. **Figure 6** shows the surface morphology of the rolling calibers before and after running the wire rolling exponents.

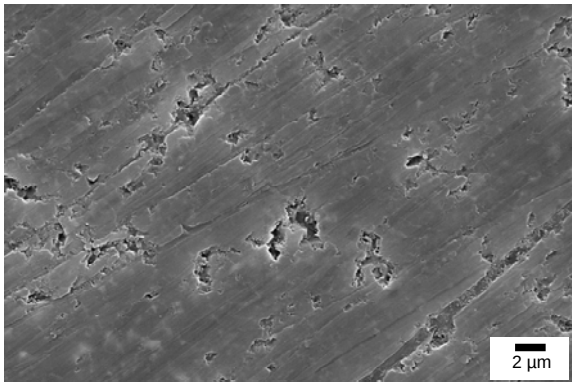

R_a [µm]	R_z [µm]
0.37±0.05	1.13±0.15

(a)

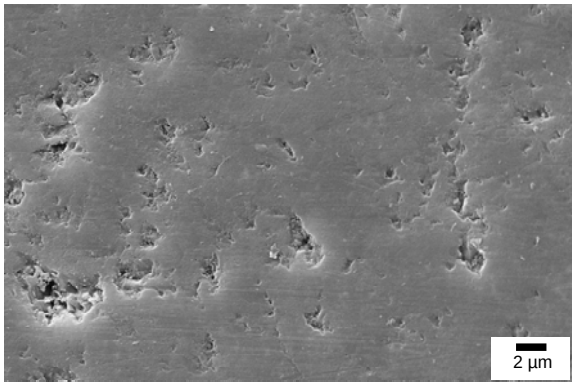

R_a [µm]	R_z [µm]
0.36±0.05	0.51±0.03

(b)

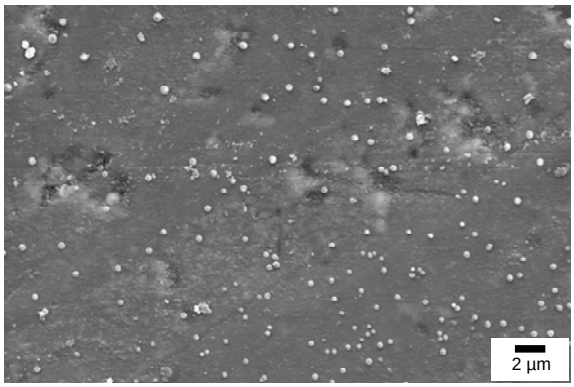

R_a [µm]	R_z [µm]
0.35±0.05	0.42±0.01

(c)

Figure 6. SEM micrographs showing the caliber surface in: (a) a virgin specimen, (b) an etched specimen after rolling 2000 m of copper wires without lubrication; (c) a specimen after rolling 2000 m of copper wires with lubrication, this close-up shows copper nanoparticles on the surface. All roughness measurements were carried out on etched specimens

It can be clearly seen from the figure that the silicon nitride surface looks smoother after running the tests. Grinding striations and polishing scars, apparent in the virgin specimens, are no more visible after rolling. The

SEM images clearly show that surface microspalls were blunted, i.e., pits generated by spalled-off material appeared to have blunt edges compared to the pits in the virgin-state specimen. No chemical pitting was observed on the surface in either lubricated or unlubricated experiments. The roughness parameters confirm the visual inspections; despite having very slight variation in the R_a value, the R_z value shows considerable drop. It is also important to notice that roughness parameters in both lubricated and unlubricated experiments are comparable.

In order to closely examine the layers superimposed on the surfaces of silicon nitride, transmission electron microscopy (TEM) foils were prepared from sample specimens. The specimens were cut from the calibers after rolling 2000 m under lubricated conditions. Scanning transmission electron microscopy (STEM) and corresponding EDX analyses were conducted. **Figure 7** shows a sample TEM-foil revealing a cross section of the caliber.

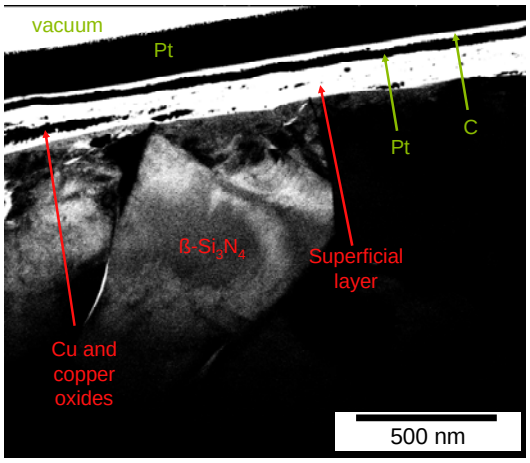

Figure 7. TEM foil showing a cross section in the caliber after rolling 2000 m under lubricated conditions. Heavy elements are shown in black, lighter elements in white

The EDX analysis (spectra not shown here) revealed copper (and copper oxides) particles irregularly distributed on the surface as expected. These sparse particles appear embedded in a thin "superficial layer" on the surface. The EDX analysis of this superficial layer indicated higher content of oxygen compared to bulk material (24.5 wt. % in comparison to 6 wt. % in the bulk). This indicates the formation of a silica layer on the surface of silicon nitride.

4.2. Interface Adhesion

The work of separation is calculated for model interface systems in which the closed packed planes of Cu are parallel to the basal planes in the case of Si_3N_4 and SiO_2 substrates. The remaining degrees of freedom, i.e. the in-plane orientation between the metal and ceramic are determined as follows. First, a sequence of calculations with a single adsorbed Cu atom on the (0001) basal surface β-Si_3N_4 were performed using only the Ewald energy (i.e., the electrostatic contribution) to the total energy, in order to find the most favorable adsorption sites for the metal

film on the Si_3N_4 substrate. The resulting locations with the lowest energies were identified to be those located above nitrogen atoms and on high symmetry positions as shown in **Figure 8a**. This can be described as (0*u*, 0*v*), (1/3*u*, 1/3*v*), (1/3*u*, 2/3*v*), (2/3*u*, 1/3*v*), and (2/3*u*, 2/3*v*) where *u* and *v* are the in-plane basis vectors of the supercell. Total energy calculations were then performed for these locations, in order to confirm the results based on the Ewald energy. Consequently, the Cu (111) plane at the interface was oriented such that the Cu atoms are located at these high symmetry minimal energy positions. A 2×2×1 repetition of the supercell is shown in **Figure 8b**, the actual supercell used in the calculations is marked by the solid line.

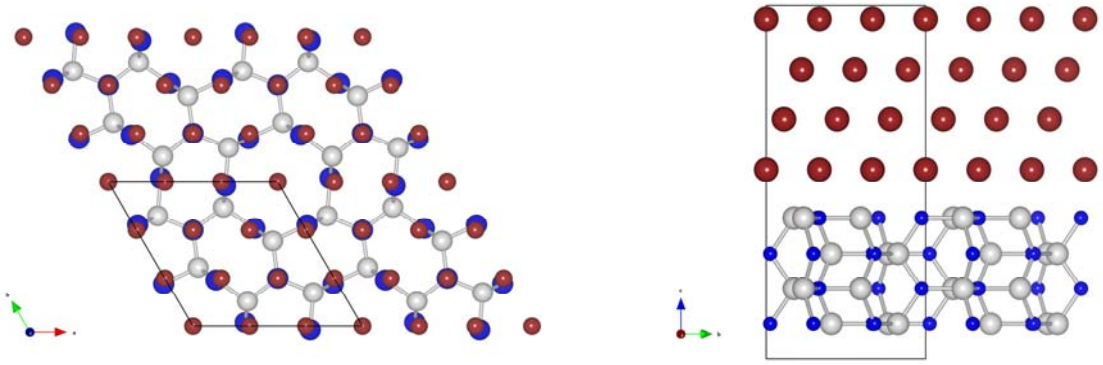

(a) (b)

Figure 8. The structure of the interface between Cu and β-Si_3N_4: (a) top view along the c-axis, and (b) side view along the $<2\bar{1}\bar{1}0>$ direction. The supercell used in the calculations is marked on the figures

These locations are consistent with an orientation relationship in which the $<01\bar{1}>$ directions in Cu are parallel to the $<2\bar{1}\bar{1}0>$ directions in the β-Si_3N_4, as shown in **Figure 8a**. A similar orientation relationship was also observed for Cu/Al_2O_3 interfaces in **[38]**.

In this orientation, there are 3×3 (111) surface unit cells of Cu on each (0001) planar unit cell of the silicon nitride. This orientation relationship results in a small misfit strain in Cu of 0.73%. A similar procedure was also employed for the case of interface between Cu and α-SiO_2, leading to the same orientation relationship as shown in **Figure 9a**. Here, 2×2 (111) unit cells of Cu are fitted on a 1×1 unit cell of SiO_2, resulting in a misfit strain of 2.35% in the Cu. It should be noted that although this procedure does not guarantee that our translation states (orientation relationships) are the ones which are most stable, it does however, lead to reasonable stable interface models, which do not impose large misfit strains on the Cu. In each case the stoichiometric termination of the ceramic was considered. For the Cu/Fe interface model, a 1×1 unit cell of (111) Cu is fitted on a 1×1 unit cell of (111) γ-Fe. The resulting lattice mismatch is 4.4% for the Cu film.

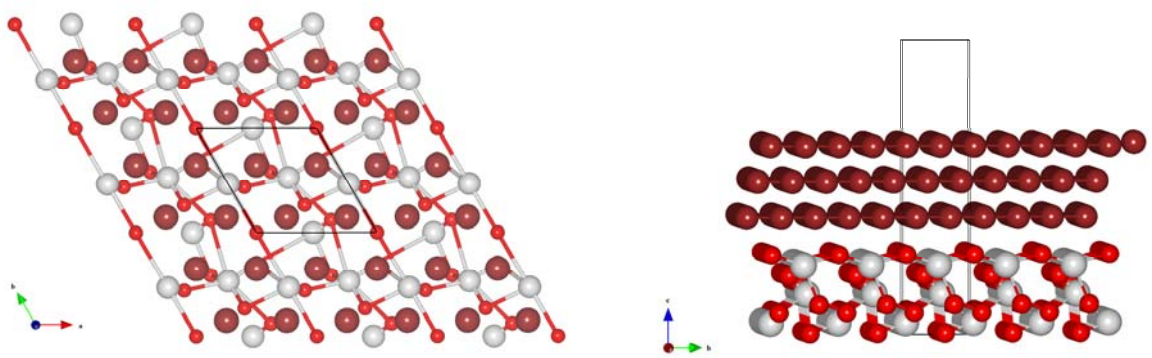

(a) (b)

Figure 9. The structure of the interface between Cu and α-SiO_2: (a) a top view along the c-axis, and (b) side view along the $<2\bar{1}\bar{1}0>$ direction. The supercell used in the calculations is marked on the figures

For each of the systems, total energy calculations for the interface system at difference distances between the metal and ceramic were carried out. **Figure 10** shows the negative of the work of separation (i.e., the interface energy) as a function of the interface separation distance between the Cu and β-Si_3N_4. The data points are then fit to the equation of state **[39,40]**.

The minimum gives the equilibrium value of the work of separation and the interfacial distance between the metal and substrate. The results for the work of separation obtained for the bulk interfaces are listed in **Table 3**.

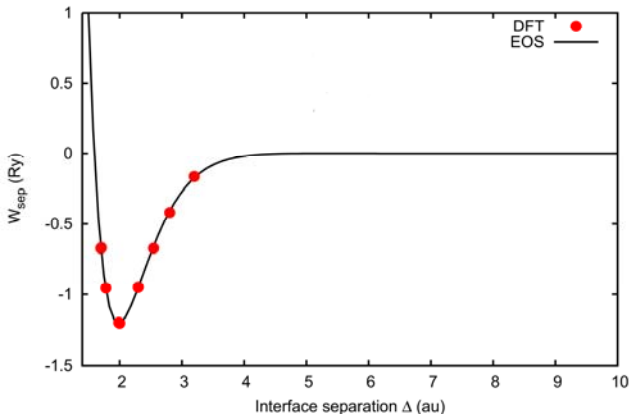

Figure 10. The negative of the work of separation curve as a function of interface separation between Cu and β-Si_3N_4. The curve is the fitted equation of state. The work of separation for this interface is obtained from the minimum of the curve. The interface separation is given in atomic units (1 au = 0.529 Å, 1 Ry=13.6 eV)

Table 3. The work of separation, W_{sep} obtained from the DFT calculations for the various interface systems

System	Work of separation (W_{sep}) [J/m²]
Cu (111) / β-Si_3N_4 (0001)	2.72
Cu (111) / α-SiO_2 (0001)	4.10
Cu (111) / γ-Fe (111)	4.00
Cu / [Cu ML , γ-Fe (111)]	3.30
Cu (111) / Cu (111)	3.08

As shown in **Table 3**, the lowest work of separation is obtained for the Cu (111) / β-Si_3N_4 (0001) interface system. For the Cu (111) / α-SiO_2 (0001), and Cu (111) / γ-Fe (111) systems, the work of separation is almost equal, and larger by more than 1 J/m² than the work of separation between Cu and β-Si_3N_4. The W_{sep} obtained for the Cu (111) / α-SiO_2 (0001) is consistent with the values obtained by Nagao et al. **[41]** for Cu (001) on oxygen-rich (001) surface of α-cristobalite suggesting that the interaction between Cu and O is the dominant bonding one.

During the rolling process, a chemical reaction between the roll and the Cu wire may result, and hence it is important to verify whether the binding energy between the Cu and roll is stronger than that in the bulk of Cu. The energy to cleave the copper along a (111) plane was calculated previously **[15]** to be 3.08 J/m², hence it is slightly larger than that between Cu and Si_3N_4, but is smaller than that between Cu and SiO_2, suggesting that during the roll process, residues of Cu on the SiO_2 are more likely to occur than on clean Si_3N_4 surface. The same is also obtained for steel-based rolls, as the W_{sep} between Cu and γ-Fe (i.e., Cu (111) / γ-Fe (111) system) is larger than that in bulk Cu. The work of separation for cleaving the interface of one layer of Cu above the interface (Cu / [Cu ML, γ-Fe (111)]) was also explicitly calculated, i.e., a cleavage in which one layer of Cu remains adsorbed on the γ-Fe surface. The resulting work of separation as shown in **Table 3**, is slightly larger than that for cleaving in the interior of Cu, and still smaller than cleaving at the interface. Despite the low adhesion affinity observed in the Cu/β-Si_3N_4 system, the Cu/SiO_2 system rendered high interface energy that reached about 4.1 J/m².

5. Case study

Figure 11 shows an example, wherein silicon nitride rolls used in copper wire rolling were prematurely removed from service. The Si_3N_4-rolls was manufactured by (H. C. Starck Ceramics, Germany) and tested in an industrial rolling mill at (Lacroix und Kress GmbH, Germany). In this process, the rolls were used to roll wires from 25 mm cross-sectional diameter to 16 mm at a feed rate of 6 mm/s and a rolling temperature of 800 to 850 °C. The rolls were sent to the Fraunhofer Institute for Mechanics of Materials IWM for examination and damage analysis.

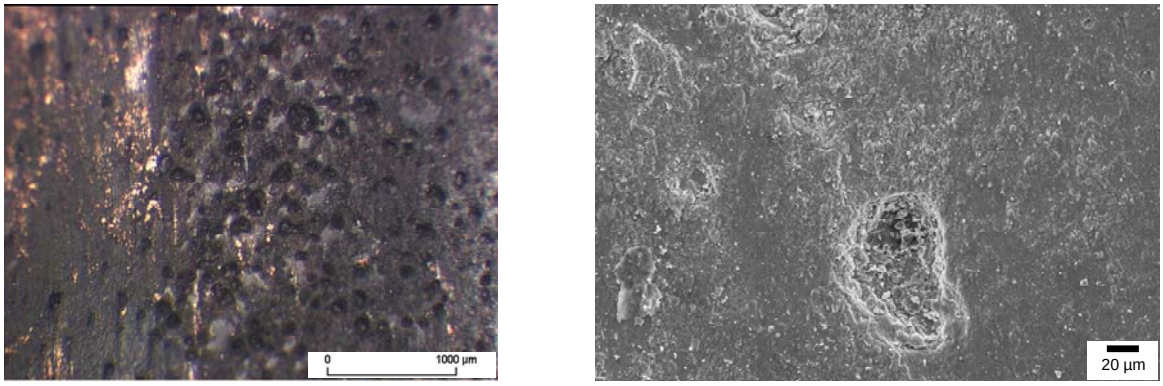

(a) (b)

Figure 11. (a) Optical micrograph showing corrosive pitting and copper adhesion on the surface of a silicon nitride roll; (b) SEM micrograph showing a close-up of the corrosive pitting

As seen in the figure, the visual inspections revealed significant copper transfer and formation of microscopic corrosive pitting on the rolling surfaces. Comparative roughness measurements with virgin specimens indicated an increase in the caliber surface roughness. The damage was accounted to grain boundary phase corrosion in silicon nitride due to tribochemical mechanisms.

An EDX analysis was carried out to compare the bulk material with pitting sites (**Figure 12**).

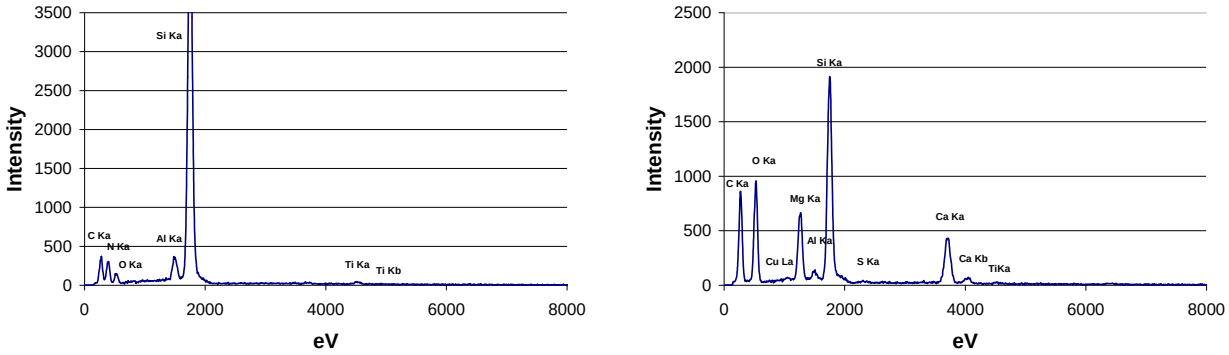

(a) (b)

Figure 12. EDX analysis of (a) the bulk silicon nitride material; (b) surface pitting sites. Data truncated at 8 keV, beyond which no peaks were detected

The analysis of the bulk material revealed Si, N, O and 3.5 wt.% Al from the silicon nitride system, in addition to ca. 1 wt.% Ti. The analysis carried out at pitting sites showed higher concentration of O (29.7 wt.% in comparison to 5.3 wt.% in the bulk), in addition to 6.8 wt.% Mg, 10.9 wt.% Ca and a weak signal of 0.3 wt.% S. The concentration of Cu in pitting sites was found to be less than 0.1 wt.%. Mg, Ca and S stem from the applied cooling lubricant; this was verified by means of an inductively coupled plasma atomic emission spectroscopy (ICP-OES) that was carried out to quantitatively analyze its composition.

An EDX mapping was performed at pitting sites after preparing ceramographic polished cross sections at several locations within the caliber. The EDX maps of selected elements are shown in **Figure 13**.

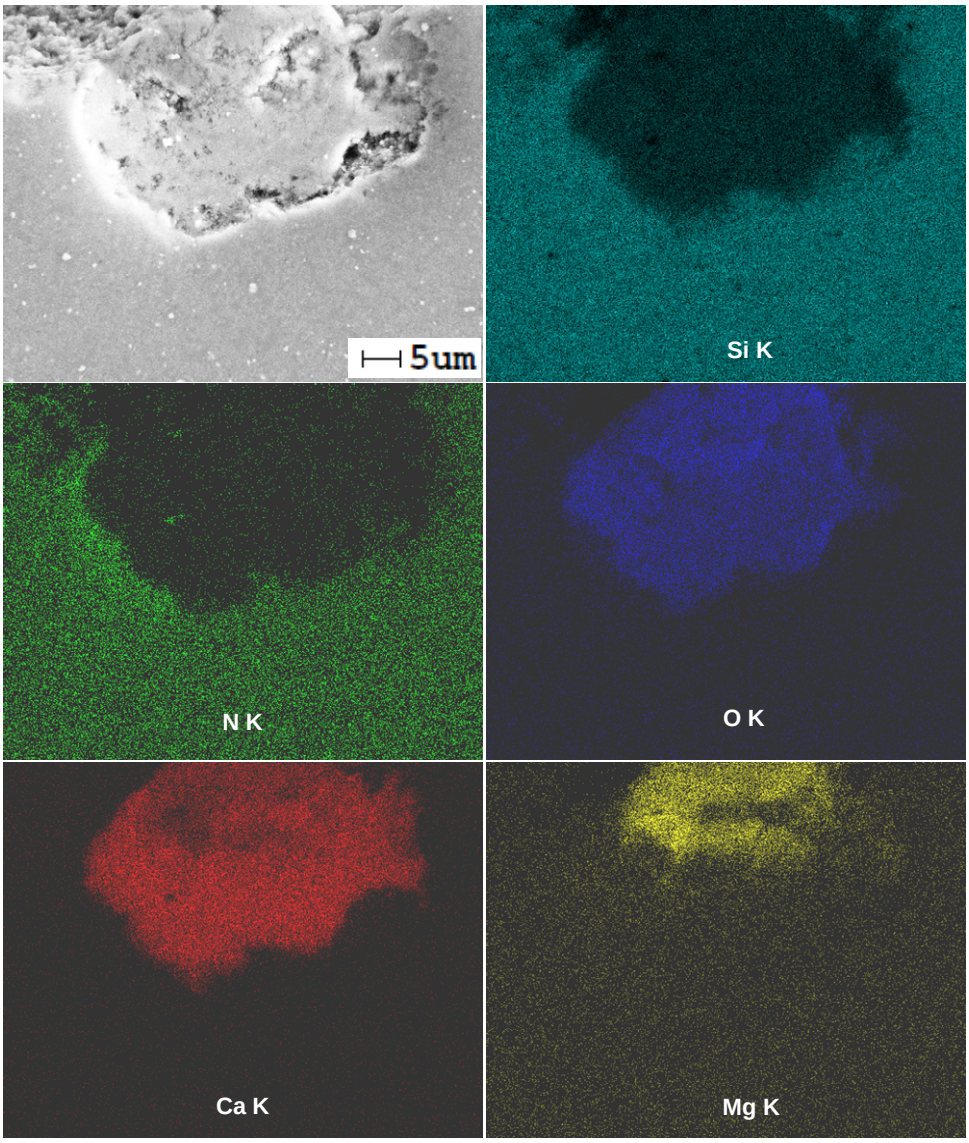

Figure 13. SEM and EDX-mapping (15 kV) at a surface pitting site. Brighter spots indicate higher element concentration

The EDX mapping reveals low concentrations of Si within the corrosion sites (what can be described as reaction products on the surface) in comparison to the bulk material. It also indicates high concentrations of Mg and Ca. Comparing the distribution of O and N within the pitting sites, it is evident that the reaction products consist of oxides rather that nitrides. The low signal-to-noise ratio of sulfur rendered non-conclusive results concerning its distributions within these zones. Consequently, a more sophisticated method was adopted to

investigate the existence of sulfur within the pitting sites; focused-ion beam (FIB)-milled sections were prepared to study the material in the vicinity of pitting sites and in the near-surface zones, as shown in **Figure 14**.

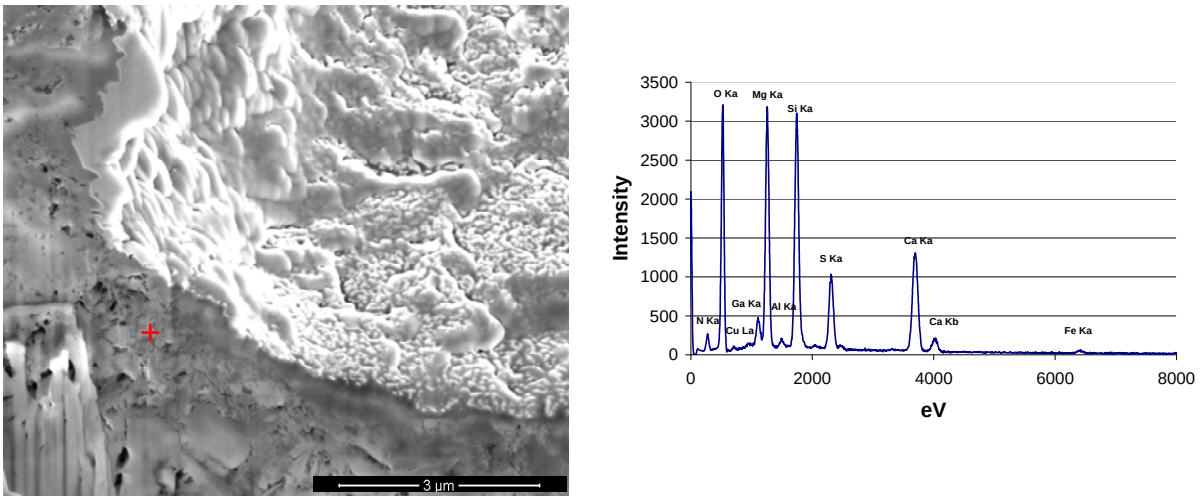

(a) (b)

Figure 14. (a) FIB-milled section at a pitting site showing a near-surface material degradation zone; (b) corresponding EDX analysis (20 kV), located by the cross in the SEM image. Ga and Fe in the EDX originate from the FIB-unit

The FIB-assisted cross-sectional examination, shown in **Figure 14a**, depicts a zone of material degradation below the surface of a pitting site. To investigate the corrosive effects on the silicon nitride material system, FIB-polishing succeeded the cross section FIB-milling procedure. It was, however, not possible to achieve highly polished cross-sectional surfaces, in which Si_3N_4-grains are distinguishable from the secondary phase – despite being a standard procedure in highly dense silicon nitride materials. Correlating the SEM image with the corresponding EDX analysis, and considering the low intensity of nitrogen within the near-surface degradation zone, it can be shown that the upmost layers also contains oxides rather than nitrides. In **Figure 14b** the corresponding EDX analysis shows a distinct sulfur peak in addition to the previously detected Mg and Ca peaks. An EDX-line scanning in the depth also showed that the intensity of sulfur increases at 2 µm below the surface.

6. Discussion

Under the influence of shear stresses and friction forces at the roll/wire interface, copper particles detach from the wire and transfer onto the surface of the rolls. This can be thought of as a wear process in the wire due to combined sliding and adhesive wear mechanisms. Under dry conditions, the transferred metal particles accumulated on the rolling caliber creating a superimposed artificial profile (**Figure 4**), which resulted in the deterioration of the surface quality of the rolled wires. It was noticed that applying small amounts of diluted cooling lubricant (5% mineral oil in water emulsion) significantly reduced the metal accumulation from tribofilms and agglomerates to only sparse nanoparticles on the surface (compare **Figure 5** with **Figure 6c**). These

observations confirmed that the metal transfer was highly influenced by friction between the roll and wire in what can be considered as a tribomechanical mechanism. Nevertheless, these results are also in agreement with the first-principles calculations, which indicate possible adhesion between the Cu and the Si_3N_4, leading to the formation of small agglomerates of Cu on the roll surface. Applying lubrication weakens this adhesion and therefore, results in cleaner roll surfaces.

Lubrication and/or the existence of tribofilms on the surface of silicon nitride, eventually results in contact surface segregation. The effect of surface segregation tends to reduce sliding wear on the silicon nitride surface; meanwhile, the resulting copper/copper contact leads to less two-body abrasive wear on the wire couterface. This proposes an explanation to the minuscule change in surface roughness recorded after rolling (**Figure 6**). Nevertheless, the surface roughness measurements of etched silicon nitride specimens allowed a tentative suggestion of mild wear due to continuous adhesion and detachment between the ceramic and metallic surfaces. The SEM morphological examinations clearly revealed a tribologically influenced ceramic surface, which can be correlated to accelerated tribochemical mechanisms at such high temperatures. This latter point can be explained by considering the numerical calculations.

Comparing the work of separation obtained from the atomistic calculations, it can be seen that the interface energy between a Cu (111)-monolayer and β-Si_3N_4 (2.35 J/m^2) is very low in comparison to a system consisting of two metals in contact. Analogously, the calculations showed that the interface energy between Cu and Fe is so high, that Cu adhesion on Fe is to be expected. An important factor to take into account here is that, the adhesion affinity of a Cu monolayer on Fe is higher than the adhesion affinity in the bulk of a Cu system. This indicates that it is highly probable that copper residues will be left on the surface of steel-based rolls. This is corroborated by observations from industrial rolling applications in which the high adhesion affinity between copper and steel-based tools has been documented **[8]**. It should be, however, mentioned that the inner separation energy between Cu and β-Si_3N_4 based on Cu (111) monolayers and β-Si_3N_4 as well as the separation energy between Cu and complex systems such iron and chrome oxides and hydroxides are not available, yet.

On the other hand, the Cu/SiO_2 system rendered high interface energy that reached about 4.1 J/m². The silica layer formed on the silicon nitride surface (**Figure 7**) can be thought of as a protective layer. The strong adhesion affinity (or even possible chemical interaction) between copper and SiO_2, assists detaching the latter off the surface of silicon nitride. This temperature assisted process can be considered as one of the dominant wear mechanisms in silicon nitride tools applied in copper rolling.

In recent related works **[42,43]**, it was shown by means of finite element modeling that high contact-surface temperatures are expected on silicon nitride in copper wire rolling. The high heat transfer conduction coefficient of copper contributes to this phenomenon. The computed surface temperature reached ca. 470 °C at a rolling temperature of 600 °C, and increased to 640 °C at a rolling temperature of 825 °C. An important factor to take into account is that high rolling temperatures might accelerate the rate of oxidation of silicon nitride and might contribute to the aforementioned tribochemical effects. Additionally, the finite element simulations highlighted the role of friction and its accompanying interfacial shear stresses as a crucial factor in the formation of metallic buildup transfer layers on the roll surfaces.

Considering the case study, the rolling process was carried out at rolling temperatures reaching 850°C in a sulfur-oxygen rich environment. The corrosion of silicon nitride in environments containing sulfur and oxygen has been well documented. Din and Ullah **[44]** reported that sulfur dioxide reacts with Si_3N_4 to form SiO_2. In a $MgO\text{-}SiO_2$ or $CaO\text{-}SiO_2$ oxide system the liquidus temperature of SiO_2 is dependent on the of the oxide contents, which eventually leads to higher susceptibility to corrosion at lower temperatures. It should be also kept in mind that the chemical system present in rolling contains water, which might have an effect on the solubility of SiO_2. Wang et al. **[45]** have shown that in a sulfur-oxygen-rich environment, the corrosion of silicon nitride follows a parabolic law, whereas, the corrosion mechanisms are temperature-dependent between 1150 and 1350 °C. It was shown that the diffusion of additives and impurities to the grain boundaries of silicon nitride and to the outer surface layers lead to the formation of corrosive pitting.

Despite the lower surface temperatures encountered during rolling, the relatively high contact pressure occurring at the wire-roll interface might explain the corrosive reaction in the case study. The experiments, however, were carried out even at a lower temperature (ca. 600°C), which suggests an explanation regarding the absence of any detectable corrosive reaction.

Based on these results, damage mechanisms and adhesion between copper and silicon nitride can be explained. In hot rolling copper wires, the high contact surface temperature leads to the formation of a protective silica layer on the ceramic surface, which separates the sliding surfaces and prevents direct contact between copper and Si_3N_4. Due to continuous contact between hot wires and the surface of the tools, and under the effect of adhesive wear and tribomechanical factors (e.g., shear stresses), this protective silica layer will continuously be detached, thereby, resulting in relatively high tribochemical wear of the ceramic tools. The tribochemical and tribomechanical wear observed throughout the experiments can be described as favorable. These effects result in the formation of highly polished rolling surfaces. However, the existence of lubricant additives in the systems, e.g., sulfur-compounds, apparently result in accelerating the corrosive reaction, and thereby, formation of corrosive pitting at sufficiently high temperatures. This eventually results in the deterioration of the ceramic surface integrity. The existence of high concentrations of Mg and Ca in the system (refer to **Figure 13**) could be traced to trapped cooling lubricant in the pores, such products, however, might have an effect on the rate of corrosive reaction. It should be also kept in mind that the surfactants that are used in the cooling lubricants may adsorb better on metallic surfaces than on ceramics; thus, the protective lubricant layer on the ceramic surface may be too weak to completely prevent adhesion of copper.

Due to the considerable complexity of modeling more realistic structures using first-principles methods, the effect of environmental aspects was not taken into consideration in the current study. The influence of the silicon nitride material system, i.e., secondary phase composition and additives, was not incorporated within the simulations. An optimization of the process requires fundamental understanding of the nature of interaction between the wire and roll as a function of the environmental parameters. In particular, in the presence of a cooling lubricant and surface cleaning agents, which lead to impurity entrapment within the roll gap; the need for such elaborations is, however, acknowledged.

7. Summary and conclusions

In this study, the degree to which the chemical bonding, at atomically smooth interfaces, reflects the empirical trends in the adhesion of Cu contacts to the roll material was assessed. This was accomplished through studying a simplified model system. The interaction between the solid metal and the roll surface was investigated using first-principles quantum mechanical calculations within the density functional theory (DFT). The adhesion energy gives direct information on the tribological aspects which relate to the degradation mechanism.

At high surface temperatures, as expected in copper wire rolling, the SiO_2 layer formed on the silicon nitride surface can be thought of as a protective layer. The strong adhesion affinity between copper and SiO_2, assists detaching the latter off the surface of silicon nitride. This temperature assisted process is considered one of the dominant wear mechanisms in copper wire rolling using silicon nitride tools.

Acknowledgements

We gratefully acknowledge the financial support of the German Federal Ministry for Education and Research BMBF, Grant No. 03X3503, and of the German Research Foundation DFG, Grants no. GU367/24-2 and SFB483/4-2009 TPA7. The authors owe special thanks to both Professor Peter Gumbsch and Professor Christian Elsässer for their constant support and fruitful discussions.

References

[1] M. Lengauer, R. Danzer, Silicon nitride tools for hot rolling high alloyed steel and super-alloy wires – Crack growth and lifetime prediction, J. Eur. Ceram. Soc. 28 (2008) 2289-2298.

[2] R. Danzer, M. Lengauer, Silicon nitride materials for hot working of high strength metal wires. Eng. Fail. Anal. 17 (2010) 596-606.

[3] T. Hollstein, Walzen mit Keramik – Anwendungsspektrum und Projektüberblick, in: A. Kailer (Eds.), Walzen mit Keramik. Fraunhofer Verlag, ISBN 978-3-8396-0033-7, 2009, pp.7-22.

[4] G. Akdogan, T.A. Stolarski, Wear in metal/silicon nitride sliding pairs, Ceram. Int. 29 (2003) 435-446.

[5] R. Klein, M. Desmaison-Brut, P. Ginet, A. Bellosi, J. Desmaison, Wettability of silicon nitride ceramic composites by silver, copper and silver copper titanium alloys, J. Eur. Ceram. Soc. 25 (2005) 1757-1763.

[6] R. Sangiorgi, M.L. Muolo, A. Bellosi, Wettability of hot-pressed silicon nitride materials by liquid copper, Mater. Sci. Eng., A 103 (1988) 277-283.

[7] R. Sangiorgi, A. Bellosi, M.L. Muolo, G.N. Babini, Corrosion of hot pressed silicon nitride-based materials by molten copper, J. Mater. Sci. 24 (1989) 4080-4087.

[8] G. Wötting, H. Drachsler, H.-J. Pohlmann, Werkstoffqualifizierung und Bauteilherstellung, in: A. Kailer, T. Hollstein, (Eds.), Walzen mit Keramik, Fraunhofer IRB-Verlag, ISBN 3-8167-6462-2, 2004, pp. 23-35.

[9] N. Benouattas, A. Mosser, D. Raiser, J. Faerber, A. Bouabellou, Behaviour of copper atoms in annealed $Cu/SiO_x/Si$ systems, Appl. Surf. Sci. 153 (2000) 79-84.

[10] N. Eustathopoulos, N. Sobczak, A. Passerone, K. Nogi, Measurement of contact angle and work of adhesion at high temperature, J. Mater. Sci. 40 (2005) 2271-2280.

[11] J. Adams, L. Hector, D. Siegel, H. Yu, J. Zhong, Adhesion, lubrication and wear on the atomic scale, Surf. Interface Anal. 31 (2001) 619-626.

[12] P. Hohenberg, W. Kohn, Inhomogeneous Electron Gas, Phys. Rev. 136 (1964) B864–B871

[13] W. Kohn, L. J. Sham, Self-Consistent Equations Including Exchange and Correlation Effects, Phys. Rev. 140, (1965) A1133–A1138.

[14] S. Köstlmeier, C. Elsässer, Ab-Initio Investigation of Metal-Ceramic Bonding:M(001)/$MgAl_2O_4$(001), M=Al, Ag, Interface Science 8 (2000) 41-54.

[15] A. Hashibon, C. Elsässer, M. Rühle, Structure at abrupt copper-alumina interfaces: An ab initio study, Acta Mater. 53 (2005) 5323-5332.

[16] J.-M. Albina, M. Mrovec, B. Meyer, and C. Elsässer, Structure, stability, and electronic properties of $SrTiO_3$/$LaAlO_3$ and $SrTiO_3$/$SrRuO_3$ interfaces, Phys. Rev. B 76 (2007) 165103.

[17] A. Hashibon, C. Elsässer, Y. Mishin, and P. Gumbsch, First-principles study of thermodynamical and mechanical stabilities of thin copper film on tantalum, Phys. Rev. B 76 (2007) 245434.

[18] S.B. Sinnott, E.C. Dickey, Ceramic/metal interface structures and their relationship to atomic- and meso-scale properties, Mater. Sci. Eng., R 43 (2003) 1-59.

[19] E. Saiz, R.M. Cannon, A.P. Tomsia, High-temperature wetting and the work of adhesion in metal/oxide systems, Annu. Rev. Mater. Res. 38 (2008) 197.

[20] T. Lube, J. Dusza, A silicon nitride reference material - A testing program of ESIS TC6, J. Eur. Ceram. Soc. 27 (2007) 1203-1209.

[21] S. Fünfschilling, R. Oberacker, M.J. Hoffmann, Verhalten von Siliciumnitrid-Keramiken mit unterschiedlichen Korngrezphasen im Kontakt mit Kupfer, in: K.H. Zum Gahr, J. Schneider, (Eds.), Hochbeanspruchte Gleit- und Friktionssysteme auf Basis ingenieurkeramischer Werkstoffe, 3. Statuskolloquium Sonderforschungsbereich 483, ISBN 978-3-933733-00-9, 2007, pp. 105-112.

[22] M.W. Finnis, The theory of metal-ceramic interfaces, J. Phys.: Condens. Matter 8 (1996) 5811-5836.

[23] D.M. Ceperley, B.J. Alder, Ground state of the electron gas by a stochastic method, Phys. Rev. Lett. 45 (1980) 566.

[24] J.P. Perdew, A. Zunger, Self-interaction correction to density-functional approximations for many-electron systems, Phys. Rev. B 23 (1981) 5048.

[25] D.R.Hamann, M.Schlüter, C. Chiang, Norm-conserving pseudopotentials, Phys. Rev. Lett. 43 (1979) 1494.

[26] C. Elsässer, N. Takeuchi, K.M. Ho, C.T. Chan, P. Braun, M. Fähnle, Relativistic effects on ground state properties of 4d and 5d transition metals, J. Phys.: Condens. Matter 2 (1990) 4371.

[27] B. Meyer, K. Hummler, C. Elsässer, M. Fähnle, Reconstruction of the true wavefunctions from the pseudowavefunctions in a crystal and calculation of electric field gradients, J. Phys.: Condens. Matter 7 (1995) 9201-9217.

[28] F. Lechermann, F. Welsch, C. Elsässer, C. Ederer, M. Fähnle, J.M. Sanchez, B. Meyer, Density-functional study of Fe3Al: LSDA versus GGA, Phys. Rev. B 65 (2002) 132104.

[29] F. Lechermann, M. Fähnle, B. Meyer, C. Elsässer, Electronic correlations, magnetism, and structure of Fe-Al subsystems: An LDA+U study, Phys. Rev. B 69 (2004) 165116.

[30] D. Vanderbilt, Optimally smooth norm-conserving pseudopotentials, Phys. Rev. B 32 (1985) 8412.

[31] H.J. Monkhorst, J.D. Pack, Special points for Brillouin-zone integrations, Phys. Rev. B 13 (1976) 5188.

[32] T. Kurushima, K. Ishizaki, Reaction of copper and copper oxides with nitride ceramics (AlN, SiAlON, Si_3N_4) and oxide additives (Al_2O_3, Y_2O_3, SiO_2, MgO), J. Ceram. Soc. Jpn. 100 (1992) 955-959.

[33] S. Ogata, N. Hirosaki, C. Kocer, Y. Shibutania, A comparative ab initio study of the ‘ideal’ strength of single crystal α- and β-Si_3N_4, Acta Mater. 52 (2004) 233.

[34] P. Vashishta, R.K. Kalia, J.P. Rino, I. Ebbsjo, Interaction potential for SiO_2: A molecular-dynamics study of structural correlations, Phys. Rev. B 41(1990) 12197-12209.

[35] O. Borgen, H.M. Seip, The Crystal Structure of β-Si_3N_4, Acta Chem. Scand. 15 (1961) 1789.

[36] L. Levien, C.T. Prewitt, D.J. Weidner, Structure and elastic properties of quartz at pressure, Am. Mineral. 65 (1980) 920-930.

[37] A. Hashibon, P. Schravendijk, C. Elsässer, P. Gumbsch, Atomistic study of structure and stability of thin Ni films on Fe surfaces, Philos. Mag. 89 (2009) 3413-3433.

[38] S.H. Oh, C. Scheu, T. Wagner, M. Rühle, Control of bonding and epitaxy at copper/sapphire interface, Appl. Phys. Lett. 91 (2007) 141912.

[39] J.H. Rose, J. Ferrante, J. R. Smith, Universal binding energy curves for metals and bimetallic interfaces, Phys. Rev. Lett. 47 (1981) 675.

[40] J.H. Rose, J.R. Smith, F. Guinea, J. Ferrante, Universal features of the equation of state of metals, Phys. Rev. B 29 (1984) 2963.

[41] K. Nagao, J.B. Neaton, N.W. Ashcroft, First-principles Study of adhesion at Cu/SiO_2 interfaces, Phys. Rev. B 68 (2003) 125403.

[42] I. Khader, S. Fünfschilling, A. Kailer, R. Oberacker, The behavior of silicon nitride tools in hot rolling copper wire, in: A. Fischer, K. Bobzin, (Eds.), Friction, Wear and Wear Protection, Wiley-VCH, Weinheim, ISBN 978-3-527-32366-1, 2008, pp.383-392.

[43] I. Khader, Damage mechanisms in silicon nitride rolling tools applied in caliber rolling copper and steel wires, PhD Dissertation, Karlsruhe Institute of Technology, Shaker Verlag, ISBN 978-3-8322-9389-5, Nr. 062, 2010.

[44] S.U. Din, S. Ullah, Corrosion of hot-pressed silicon nitride by potassium oxide and sulphur dioxide vapours, Mater. Lett. 31 (1997) 141-144.

[45] X. Wang, K.-n. Sun, J. Li, X.-g. Yu, Y.-s. Yin, L.-x. Yang, High temperature corrosion of silicon nitride composite ceramics in sulfur-oxygen environments, Trans. Nonferrous Met. Soc. China Vol.13 (2003) 53.